AD-A120 427 MONOPULSE ANGLE ESTIMATION FROM COHERENTLY INTEGRATED RADAR SIGNALS(U) MASSACHUSETTS INST OF TECH LEXINGTON LINCOLN LAB R E NICHOLLS 25 AUG 82 TR-619 1/1

UNCLASSIFIED ESD-TR-82-077 F19628-80-C-0002 F/G 17/9 NL

END

FILMED

DTIC

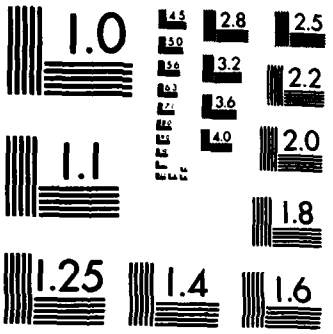


MICROCOPY RESOLUTION TEST CHART
NATIONAL BUREAU OF STANDARDS-1963-A

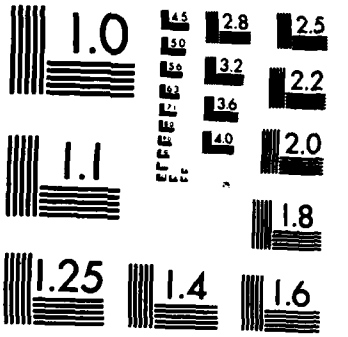


MICROCOPY RESOLUTION TEST CHART
NATIONAL BUREAU OF STANDARDS-1963-A

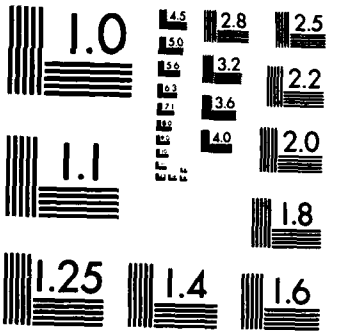


MICROCOPY RESOLUTION TEST CHART
NATIONAL BUREAU OF STANDARDS-1963-A

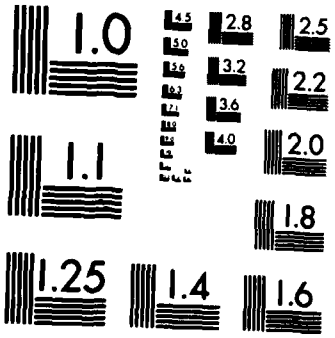


MICROCOPY RESOLUTION TEST CHART
NATIONAL BUREAU OF STANDARDS-1963-A

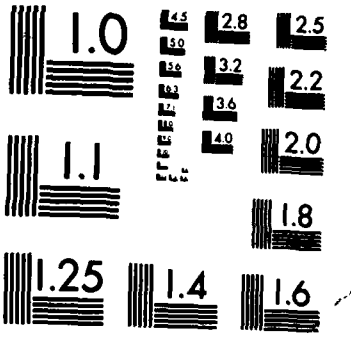


MICROCOPY RESOLUTION TEST CHART
NATIONAL BUREAU OF STANDARDS-1963-A

(12)

ESD-TR-82-077

AD A120427

# Technical Report 619

R.E. Nicholls

# Monopulse Angle Estimation from Coherently Integrated Radar Signals

DTIC ELECTE OCT 19 1982 S D F

25 August 1982

Prepared for the Department of the Army
under Electronic Systems Division Contract F19628-80-C-0002 by

**Lincoln Laboratory**
MASSACHUSETTS INSTITUTE OF TECHNOLOGY
*LEXINGTON, MASSACHUSETTS*

DTIC FILE COPY

Approved for public release; distribution unlimited.

82 10 18 109

The work reported in this document was performed at Lincoln Laboratory, a center for research operated by Massachusetts Institute of Technology. This program is sponsored by the Ballistic Missile Defense Program Office, Department of the Army; it is supported by the Ballistic Missile Defense Advanced Technology Center under Air Force Contract F19628-80-C-0002.

This report may be reproduced to satisfy needs of U.S. Government agencies.

The views and conclusions contained in this document are those of the contractor and should not be interpreted as necessarily representing the official policies, either expressed or implied, of the United States Government.

The Public Affairs Office has reviewed this report, and it is releasable to the National Technical Information Service, where it will be available to the general public, including foreign nationals.

This technical report has been reviewed and is approved for publication.

FOR THE COMMANDER

Joseph C. Syiek

Joseph C. Syiek
Acting ESD Lincoln Laboratory Project Officer

Non-Lincoln Recipients

**PLEASE DO NOT RETURN**

Permission is given to destroy this document when it is no longer needed.

MASSACHUSETTS INSTITUTE OF TECHNOLOGY

LINCOLN LABORATORY

# MONOPULSE ANGLE ESTIMATION FROM COHERENTLY INTEGRATED RADAR SIGNALS

*R.E. NICHOLLS*

*Group 38*

DT
COPY
ECTED
2

Accession For
NTIS GRA&I
DTIC TAB
Unannounced
Justification
By
Distribution/
Availability Codes
Dist | Avail and/or Special
A

**TECHNICAL REPORT TR-619**

**25 AUGUST 1982**

**Approved for public release; distribution unlimited.**

LEXINGTON MASSACHUSETTS

## ABSTRACT

A maximum likelihood estimator is derived for monopulse radar signals which have been coherently integrated. Field data from the Millstone Hill radar is reduced using the estimator and the results are compared with known values derived from an accurately computed ephemeris.

## CONTENTS


| | | |
|---|---|---|
| | ABSTRACT | |
| I. | INTRODUCTION | 1 |
| II. | DESCRIPTION OF THE PROBLEM | 2 |
| III. | ANALYSIS | 4 |
| IV. | EXPERIMENTAL RESULTS | 12 |
| V. | SUMMARY | 21 |
| | ACKNOWLEDGEMENTS | 22 |

## I. INTRODUCTION

Several radars now exist which are capable of tracking objects in deep space. With the completion of the SPADATS modifications to ALTAIR this radar will also have that capability. Deep space is an inprecisely defined term but it can be described relative to a given radar. For any given radar a satellite in deep space has the following attributes:

i) Angle rates are small and thus the period is probably 12 hours or more.

ii) The SNR is low and is probably less than 0 dB on a single pulse.

Of most importance is the low SNR which renders single pulse detection unreliable. In general, only coherent integration can be used to improve this SNR to a point where reasonable detection and false alarm probabilities can be achieved. Such integration has been used on the sum signals in all deep space tracking radars to provide target detection and range estimates. However, reduction of the tracking data to provide accurate estimates of the orbital elements of a tracked satellite also requires accurate measurements of the monopulse angles. Several ad hoc averaging methods have been used on individual radars with varying degrees of success. In this report a new estimator of the monopulse angle is derived. It is based on a method of maximum likelihood but it has its origins in an analog system known as a Normalized Angle

Error Detector. A detection algorithm falls out naturally from the derivation. Bounds on the performance of the estimator are derived in the form of a Cramer-Rao bound and this provides results which are to be intuitively expected.

As a test of the algorithm, various tracks of deep space objects were conducted by the Millstone radar. Data recorded during these tracks was reduced using the derived algorithms for estimating the monopulse error. Very close agreement was found between the computed monopulse error and the errors derived from the radar pointing and an accurate ephemeris.

## II. DESCRIPTION OF THE PROBLEM

Objects at extended range may not be detected with a single pulse as the SNR may be at or below the noise level. However, provided that the ephemeris is reasonably well known and the target is stable, several pulses may be coherently integrated to enhance the SNR sufficiently such that reliable detection is possible. The ephemeris is required in that the gathered data must be adjusted for any accelerations over the span of the data. The traditional method of integration is through a Discrete Fourier Transform (DFT) which provides coherent integrations for a set of linear phase slopes. If a detectable return is in the samples then the phase slope which most nearly approximates the actual phase slope will provide a maximum integrated signal. Failure to properly compensate for accelerations will result in a residual quadratic phase

between samples. This, in turn, will result in a spreading of the spectrum - the output of the DFT - over several cells or phase slopes.

Spreading of the spectrum may also be caused by differential motion of several radar scatterers on a satellite. This motion would be the result of rotations of the satellite. In the extreme, this motion could spread the spectral energy over all doppler cells but in the cases of interest we would expect the spread to be small when compared to the total spectral extent.

For this analysis the target will be modelled as a series of radar scatters each with a different doppler. Further, the initial phase of the return from each scatter will be random with a uniform distribution. Over the extent of the data gathering, the RCS of each scatter will be constant. As no attempt is being made to derive detection statistics, the scatterers could be considered as having a constant RCS.

For a single radar pulse, a monopulse radar derives three signals, a 'sum' and an elevation and azimuth 'difference' signal. Over some restricted range of monopulse angles, the monopulse angle - either azimuth or elevation - is proportional to the quotient of the relevant difference signal divided by the sum signal. This condition applies when the radar is in proper alignment such that, in the noiseless case, the difference signals are either in phase or 180 degrees out of phase with the sum signal. However,

in the case of returns from deep space satellites both the sum and difference channels will be masked by noise and the single pulse estimate of the monopulse angle will be meaningless.

Several approaches are available for estimating the monopulse angles but in this note a method similar to that used in an analog Normalized Angle Error Detector is used. Consider the signals shown in Fig. 1. In this case the phase of the noiseless difference signal has been increased by 90 deg. The tangent of the angle $\theta$ between the sum and the sum plus j multiplied by the difference is the monopulse ratio. Thus an estimate of $\theta$ leads to an estimate of the monopulse ratio.

## III. ANALYSIS

### A. Signal Model

Two signals shown in Fig. 1 are considered as received vectors:

$$\underline{z}_1 = [\Sigma_o + j\Delta_o, \Sigma_1 + j\Delta_1, \ldots \Sigma_{N-1} + j\Delta_{N-1}] \qquad (1)$$

and:

$$\underline{z}_2 = [\Sigma_o - j\Delta_o, \Sigma_1 - j\Delta_1, \ldots, \Sigma_{N-1} - j\Delta_{N-1}] \qquad (2)$$

where:

N is the total number of pulses

However, these signals are composed of returns from several scatters. In addition, there is a model of an underlying transmitted signal. For this analysis a constant phase difference

119790-N

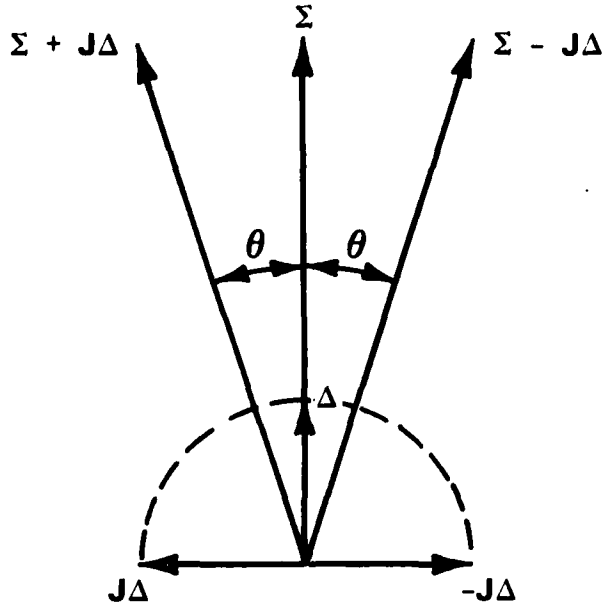


Fig. 1. Phase relations of sum and difference signals.

between pulses for each scatterer corresponding to a constant doppler is chosen. This underlying model applies to both $\underline{z}_1$ and $\underline{z}_2$. Consider K scatterers with the complex amplitude of the composite signal (sum plus or minus difference) of $\{a_K\}$. The vector of complex amplitudes is then:

$$\underline{a} = [a_o, a_1 \ldots, a_{K-1}] \tag{3}$$

This vector incorporates the amplitude and initial phase.

Each scatterer has an individual doppler which result in a constant phase shift from pulse to pulse of $\{\psi_K\}$. The characteristics may be incorporated into the matrix S where

$$S_k^n = \frac{1}{\sqrt{N}} e^{j2\pi n\psi_K} \tag{4}$$

where:

N is the number of integrated pulses

n is in the pulse index {0,1,...,N-1}

k is in the doppler index {0,1,...K-1}.

The noiseless models of the received signals are then

$$\underline{r}_1 = \underline{a}Se^{j\theta} \tag{5}$$

$$\underline{r}_2 = \underline{a}Se^{-j\theta} \tag{6}$$

B. Noise Model

Noise in the sum and difference channels should be uncorrelated. There is a component of sky and ground noise in both

signals but it is minor compared with the amplifier noise which is independently generated in each channel. Consider the noise samples in each channel.

$$n_1 = n_\Sigma + jn_\Delta \tag{7}$$

$$n_2 = n_\Sigma - jn_\Delta \tag{8}$$

The correlation is then

$$E\ n_1 n_2^* = E|n_\Sigma|^2 - E|n_\Delta|^2 + jE\ \mathrm{Re}\ n_\Sigma n_\Delta \tag{9}$$

Provided that:

$$E\ n_\Sigma n_\Delta = 0 \tag{10}$$

and:

$$E|n_\Sigma|^2 = E|n_\Delta|^2 = \sigma^2 \tag{11}$$

the correlation will be zero.

C. Maximization of the Likelihood Function

The likelihood function may be written as

$$(\underline{a},\underline{\psi},\theta) = \frac{1}{(2\pi\sigma^2)^{N/2}} \exp - \frac{1}{2\sigma^2} \left\{ \| \underline{z}_1 - \underline{r}_1 \|^2 + \| \underline{z}_2 - \underline{r}_2 \|^2 \right\} \tag{12}$$

where

$\underline{z}_1$ and $\underline{z}_2$ are the vectors of composite received signals

$\underline{r}_1$ and $\underline{r}_2$ are the signal models from Eq. (5) & (6).

A maximum likelihood estimate of the parameters is that which maximizes the likelihood function which in the case of Eq. (12) is equivalent to minimizing the exponent. Thus, the estimate is

$$L(\hat{\underline{a}},\hat{\underline{\psi}},\hat{\theta}) = \underset{\underline{a},\underline{\psi},\theta}{\text{Min}} \; \|\underline{z}_1 - \underline{r}_1\|^2 + \|\underline{z}_2 - \underline{r}_2\|^2 \tag{13}$$

Expanding Eq. (13) gives:

$$L = L_o - \sum_{m=1,2} 2 \; \text{Re} \; \underline{z}_m \underline{r}_m^* + \|\underline{r}_m\|^2 \tag{14}$$

where:

$$L_o = \|\underline{z}_1\|^2 + \|\underline{z}_2\|^2 \tag{15}$$

and:

* denotes the conjugate transpose.

The signal model may be modified by quantizing the doppler shifts into an equally spaced set with intervals of $\frac{1}{N}$ cycles. In this case the set of dopplers is completed to a full set numbering N but some of these may correspond to zero amplitude signals. Similarly, the vector of complex amplitudes is expanded to N by the possible addition of zero amplitudes. The elements of the matrix S are then:

$$S_k^n = \frac{1}{\sqrt{N}} \; e^{j2\pi nk/N} \tag{16}$$

The rows (and columns) of S now form an orthonormal system such that

$$SS^* = I \tag{17}$$

where

I is the unit matrix.

Applying this property to Eq. (14) gives:

$$\|\underline{r}_m\|^2 = \underline{a}\, SS^*\, \underline{a}^* = \|\underline{a}\|^2 \tag{18}$$

and:

$$\underline{z}_1\underline{r}_1^* = \underline{z}_1\underline{S}^*\, \underline{a}^*\, e^{-j\theta} \tag{19}$$

$$\underline{z}_1\underline{r}_1^* = \underline{z}_2\underline{S}^*\, \underline{a}^*\, e^{j\theta}\,. \tag{20}$$

The transform of the received signal is a Discrete Fourier Transform (DFT) of that signal and may be denoted as:

$$\underline{\omega}_1 = \underline{z}_1 S^* \tag{21}$$

$$\underline{\omega}_2 = \underline{z}_2 S^*\,. \tag{22}$$

Equation (14) then becomes:

$$L = L_o - 2\,\mathrm{Re}(\underline{\omega}_1\, e^{-j\theta} + \underline{\omega}_2\, e^{j\theta})\underline{a}^* + 2\|\underline{a}\|^2\,. \tag{23}$$

The function L in Eq. (23) may be minimized if the argument (phase) of $\underline{a}$ is chosen as follows:

$$\arg \underline{a} = \arg \underline{\omega}_1\, e^{-j\theta} + \underline{\omega}_2\, e^{j\theta}\,. \tag{24}$$

Substituting the result in Eq. (23) gives:

$$L = L_o - 2|\underline{\omega}_1\, e^{-j\theta} + \underline{\omega}_2\, e^{j\theta}||\underline{a}|^T + 2\|\underline{a}\|^2\,, \tag{25}$$

where: $|\underline{a}|$ is a vector of the amplitudes of the complex vector $\underline{a}$.

Noting that:

$$\|\underline{a}\|^2 = |\underline{a}|\,|\underline{a}|^T \tag{26}$$

The expression in Eq. (25) is minimized by selecting:

$$|\underline{a}| = \frac{1}{2}|\underline{\omega}_1\, e^{-j\theta} + \underline{\omega}_2\, e^{j\theta}| \tag{27}$$

Thus

$$L = L_o - \frac{1}{2}\|\underline{\omega}_1\, e^{-j\theta} + \underline{\omega}_2\, e^{j\theta}\|^2 \tag{28}$$

Expanding the second term of Eq. (28) provides:

$$\|\underline{\omega}_1\, e^{-j\theta} + \underline{\omega}_2\, e^{j\theta}\|^2 = \|\underline{\omega}_1\|^2 + \|\underline{\omega}_2\|^2 + \underline{\omega}_1\underline{\omega}_2^*\, e^{-j2\theta} \tag{29}$$

Finally, this term is maximized (and thus L is minimized) if:

$$\theta = \frac{1}{2}\arg\, \underline{\omega}_1\underline{\omega}_2^* \tag{30}$$

or

$$\tan 2\theta = \frac{\text{Im}\ \underline{\omega}_1\underline{\omega}_2^*}{\text{Re}\ \underline{\omega}_1\underline{\omega}_2^*} \tag{31}$$

Equation (31) provides a maximum likelihood estimate of the angle $\theta$ from which can be computed the monopulse ratio.

D. Doppler Detection

Not all Doppler cells within the spectrum will be occupied by targets. Thus, some threshold must be applied against the

amplitude of a particular Doppler return. An estimate of the amplitude is available (Eq. (27)) but this is dependent upon a knowledge of the angle $\theta$.

A recursive method of detection is available. If an initial estimate of zero is made for $\theta$, then Eq. (27) reduces to the traditional detection of the integrated sum channel. For those cells in which a signal is present, the sum-difference angle $\theta$ may be computed using Eq. (31). If a further refinement is required, this value of $\theta$ may be used in Eq. (27), new estimates of the amplitude made and a new threshold detection made leading to a new set of Doppler cells and a new estimate of $\theta$.

E. Bounds on the Performance of the Estimators

Estimates of several parameters are made in the process of estimating the sum-difference angle $\theta$. Each of these estimates has a fundamental limit on precision of the estimate. Lower bounds on this precision of the joint estimation process is given by Cramer-Rao bound. Applying this bound provides,

$$\sigma^2(\theta) \geq \frac{\sigma_n^2}{\|\underline{a}\|^2} \tag{32}$$

where:

$\sigma_n^2$ = noise power

$\|\underline{a}\|$ = signal power in detected Doppler cells.

This expression then reduces to:

$$\sigma^2(\theta) \geq \frac{1}{2 \cdot SNR} \tag{33}$$

which is a common expression for the performance limit of an angle detector.

## IV. EXPERIMENTAL RESULTS

The Millstone radar operates in a mode where the theory derived in previous sections is particularly applicable. Many of the satellites tracked by that radar require coherent integration to extract a signal of sufficient SNR for tracking and detection. Data from that radar has been analyzed and in the following section the results of these analyses are presented. These results appear to be accurate bearing out the usefulness of the estimator.

### A. Data Gathering

An initial track was made of an object to establish an accurate ephemeris. With this in hand, data was taken in three parts:

i) An azimuth scan from -0.3 degree to 0.3 degree at 0.1 degree steps with zero elevation offset.

ii) An elevation scan similar to the azimuth scan with zero azimuth offset.

iii) Two corner points with offsets at -0.2 degree of azimuth and elevation and 0.2 degree of azimuth and elevation.

Data in excess of 3500 points was taken at each station.

B. Processing Algorithms

At each station the data was processed with the algorithm derived in the previous section. The following narrative describes the processing:

i) For each data station and for both azimuth and elevation the derived samples of Sum + j Difference and Sum - j Difference were formed.

ii) Partitions of 512 and 1024 samples of both signals were formed and transformed using an FFT function.

iii) An initial estimate of a zero sum-difference angle was made. The amplitude of the sum of the two signals was formed and thresholded at 10 and 15 dB above a previously estimated noise level.

iv) For those spectral cells which were above threshold an estimate of the sum-difference angle was made using Eq. (31).

v) Estimates of the monopulse angle were made using the Millstone monopulse coefficient of:

$$\text{Monopulse angle} = 0.4 \tan\theta \qquad (34)$$

C. Review of Experimental Results

The processed data and the results appeared to be in accord with the predictions. Precision of the estimates is clearly dependent on the SNR and is suitably low. A biasing of the estimates appears to be present but this too is relatively small.

1. Azimuth Scans: Tables 1 and 2 show the estimates and precision for the azimuth scan detected at 15 dB above the noise. The SNR figure represents an estimate of the total SNR of the whole system, that is, the signal power divided by the relevant noise power.

It should be noted that a bias exists and that it is entirely reproduceable with the two transform size.

TABLE 1

AZIMUTH MONOPULSE ANGLES: 1024 POINT INTEGRATION

| True (deg) | Estimate (deg) | S.D. (deg) | SNR (dB) |
|---|---|---|---|
| -0.30 | -0.24 | 0.02 | 27.58 |
| -0.20 | -0.15 | 0.01 | 27.46 |
| -0.10 | -0.06 | 0.01 | 29.95 |
| 0.00 | 0.01 | 0.01 | 28.82 |
| 0.10 | 0.09 | 0.01 | 29.84 |
| 0.20 | 0.19 | 0.01 | 28.90 |
| 0.30 | 0.27 | 0.0 | 23.81 |

TABLE 2

AZIMUTH MONOPULSE ANGLES: 512 POINT INTEGRATION

| True (deg) | Estimate (deg) | S.D. (deg) | SNR (dB) |
|---|---|---|---|
| -0.30 | -0.24 | 0.03 | 25.05 |
| -0.20 | -0.15 | 0.01 | 24.53 |
| -0.10 | -0.06 | 0.01 | 24.34 |
| 0.00 | 0.01 | 0.01 | 26.67 |
| 0.10 | 0.09 | 0.01 | 23.79 |
| 0.20 | 0.19 | 0.02 | 23.23 |
| 0.30 | 0.28 | 0.03 | 23.37 |

Figure 2 gives a plot of the estimated azimuth monopulse angle. The bias term is clearly apparent. However, the bias could be reduced by modifying the slope which is equivalent to recalibrating the Millstone monopulse constant of 0.4 deg/v/v/.

2. Elevation Scans: Results very similar to those for the azimuth scan were obtained. The bias term is small and thus the recalibration would be smaller. It would also be in the opposite direction. Tables 3 and 4 show the elevation monopulse for two transform sizes and a 15 dB detection level. Figure 3 is a plot of the estimated monopulse angle.

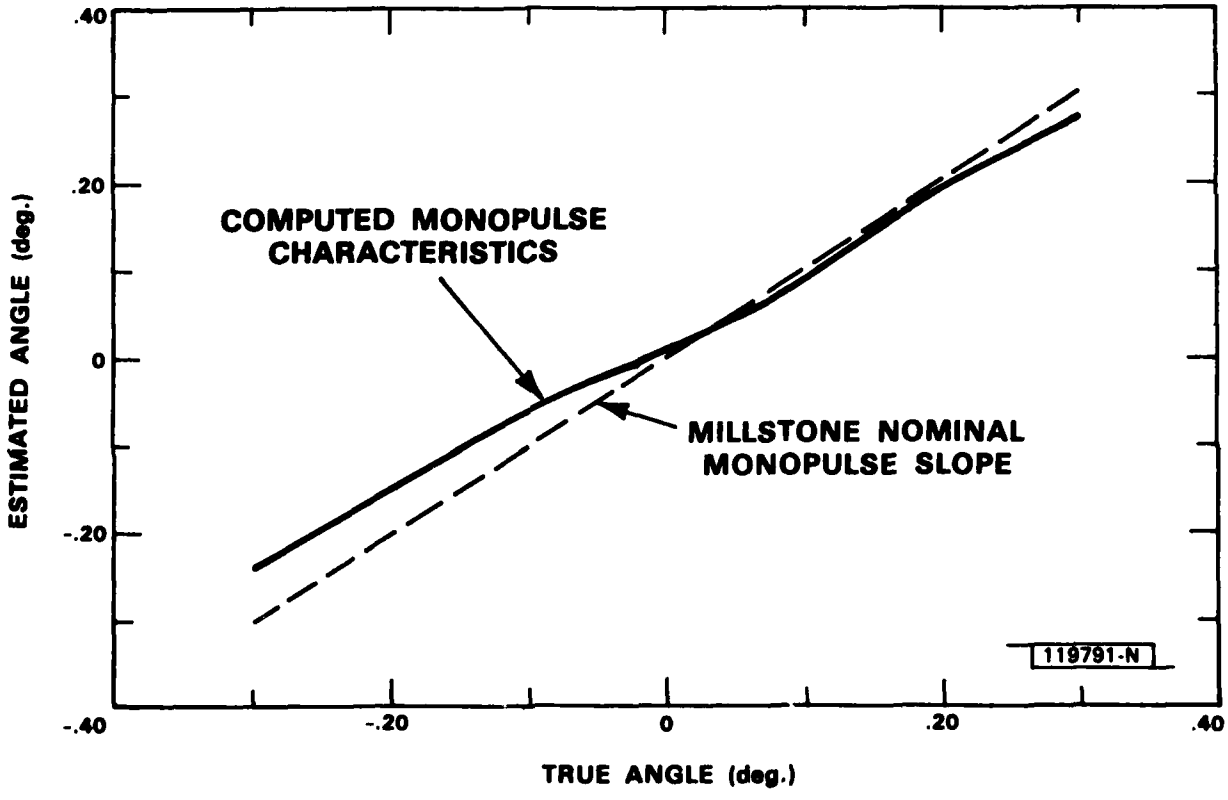


Fig. 2. Average azimuth monopulse angles: 1024 point integration.

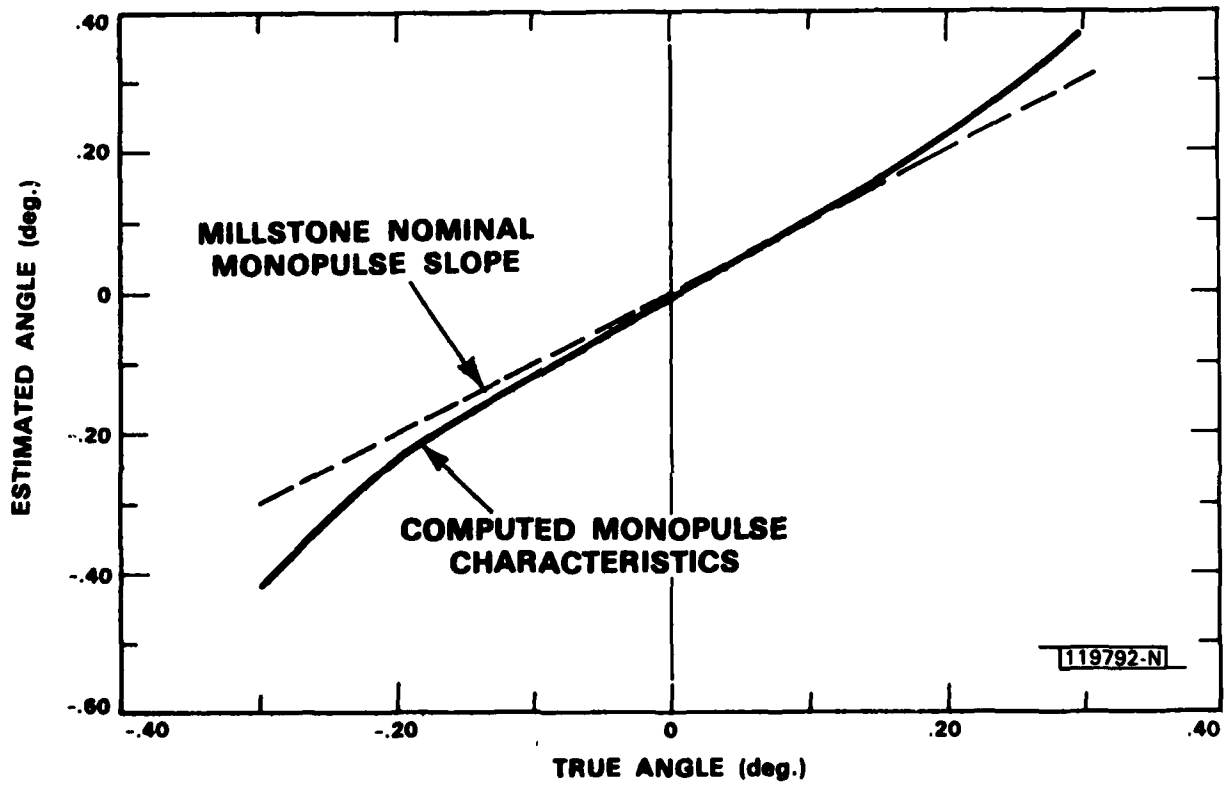


Fig. 3. Average elevation monopulse angles: 1024 point integration.

TABLE 3

ELEVATION MONOPULSE ANGLES: 1024 POINT INTEGRATION

| True (deg) | Estimate (deg) | S.D. (deg) | SNR (dB) |
|---|---|---|---|
| -0.30 | -0.42 | 0.00 | 24.95 |
| -0.20 | -0.24 | 0.01 | 28.08 |
| -0.10 | -0.12 | 0.00 | 29.39 |
| 0.00 | -0.01 | 0.01 | 28.82 |
| 0.10 | 0.10 | 0.00 | 29.12 |
| 0.20 | 0.22 | 0.00 | 25.51 |
| 0.30 | 0.37 | 0.02 | 25.24 |

TABLE 4

ELEVATION MONOPULSE ANGLES: 512 POINT INTEGRATION

| True (deg) | Estimate (deg) | S.D. (deg) | SNR (dB) |
|---|---|---|---|
| -0.30 | -0.43 | 0.03 | 22.43 |
| -0.20 | -0.24 | 0.02 | 25.06 |
| -0.10 | -0.12 | 0.00 | 26.38 |
| 0.00 | -0.01 | 0.01 | 26.67 |
| 0.10 | 0.10 | 0.01 | 26.48 |
| 0.20 | 0.21 | 0.02 | 24.92 |
| 0.30 | 0.38 | 0.01 | 21.86 |

3. Effects of Detection Threshold: Changes in the detection threshold will affect the precision of the estimate. However, the total effect will depend upon the distribution of energy in the various spectral lines. A low threshold will pick up low energy spectral lines but it will also pick up noise. Higher thresholds will restrict the number of noise returns but may also exclude signal energy.

A sample spectrum of a sum signal is shown in Figure 4. Energy is largely restricted to a small number of cells with a peak which is approximately 25 dB above the average noise floor.

For the case examined (10 dB and 15 dB thresholds) very little difference may be noticed. The same biases exist and are reproduceable. Table 5 shows the estimates for both azimuth and elevation channels.

TABLE 5

TRUE AND ESTIMATED MONOPULSE ANGLES FOR 1024 POINT INTEGRATION

| 10 dB Threshold | | | | 15 dB Threshold | | | |
|---|---|---|---|---|---|---|---|
| Azimuth | | Elevation | | Azimuth | | Elevation | |
| True | Estimate | True | Estimate | True | Estimate | True | Estimate |
| .00 | .02 | .00 | -.01 | .00 | .01 | .00 | -.01 |
| -.30 | -.24 | .00 | .01 | -.30 | -.24 | .00 | .01 |
| -.20 | -.16 | .00 | .01 | -.20 | -.15 | .00 | .01 |
| -.10 | -.06 | .00 | .01 | -.10 | -.06 | .00 | .01 |
| .10 | .09 | .00 | -.02 | .10 | .09 | .00 | -.02 |
| .20 | .19 | .00 | -.01 | .20 | .19 | .00 | -.01 |
| .30 | .28 | .00 | -.02 | .30 | .27 | .00 | -.02 |
| .00 | .00 | -.30 | -.36 | .00 | -.01 | -.30 | -.42 |
| .00 | .02 | -.20 | -.24 | .00 | .02 | -.20 | -.24 |
| .00 | .02 | -.10 | -.12 | .00 | .02 | -.10 | -.12 |
| .00 | .01 | .10 | .10 | .00 | .01 | .10 | .10 |
| .00 | .03 | .20 | .22 | .00 | .03 | .20 | .22 |
| .00 | .02 | .30 | .37 | .00 | .02 | .30 | .37 |
| .20 | .20 | .20 | .22 | .20 | .20 | .20 | .22 |
| -.20 | -.14 | -.20 | -.23 | -.20 | -.13 | -.20 | -.23 |

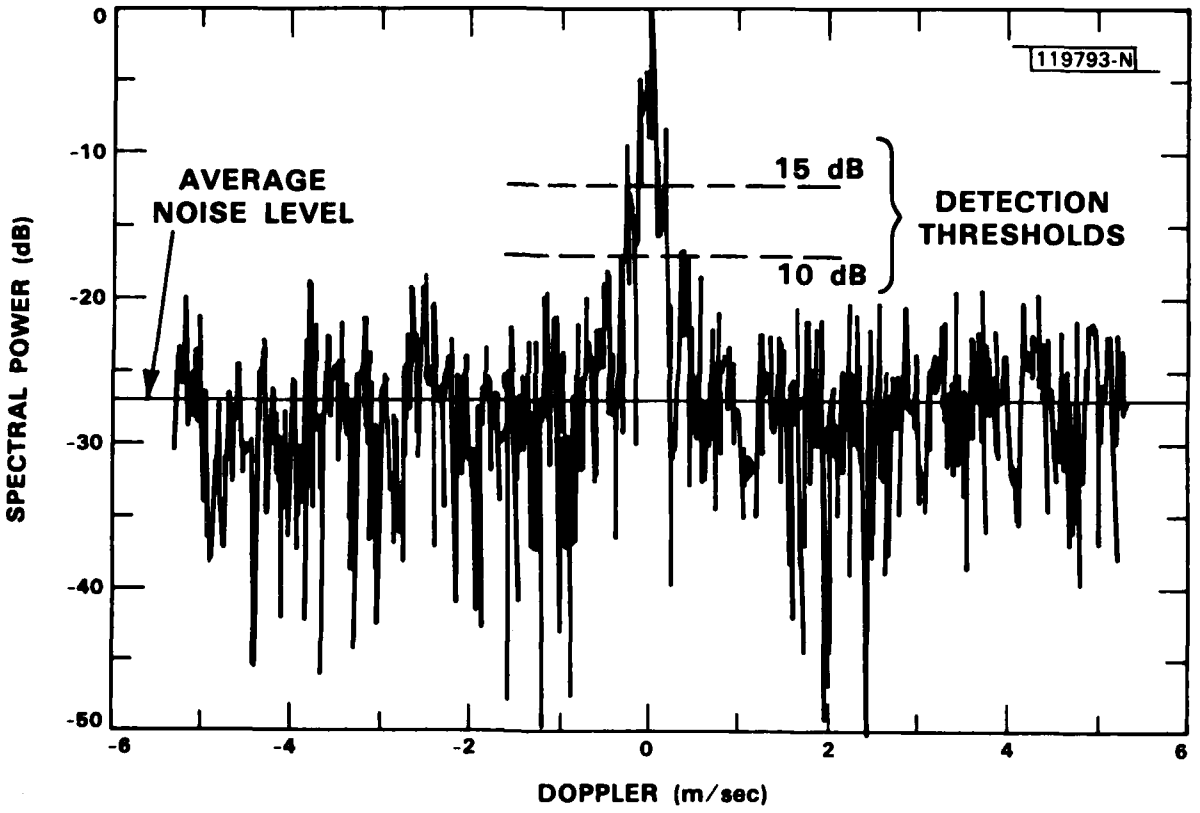


Fig. 4. Target doppler spread.

## V. SUMMARY

An estimator has been devised which combines multiple coherent radar returns (both sum and difference) to produce an estimator of the monopulse angle. The estimator is derived through maximum likelihood principles rendering it optimum in that sense. It is easily implemented using standard processing functions of FFT's and complex arithmetic.

Experimental data taken by the Millstone radar and when processed according to the derived algorithms has provided results which are reasonably accurate. However, they point to biases which are probably within the radar system but which could be removed by additional calibration.

## ACKNOWLEDGEMENTS

Discussions with Dr. E. J. Kelly, Jr., were of great assistance in clarifying the formulation of this problem. Dr. G. Banner assisted with the definition of the data requirements and arranged for the data to be gathered by the Millstone Hill radar.

UNCLASSIFIED

SECURITY CLASSIFICATION OF THIS PAGE *(When Data Entered)*

| REPORT DOCUMENTATION PAGE | | READ INSTRUCTIONS BEFORE COMPLETING FORM |
|---|---|---|
| 1. REPORT NUMBER<br>ESD-TR-82-077 | 2. GOVT ACCESSION NO.<br>AD-A120 427 | 3. RECIPIENT'S CATALOG NUMBER |
| 4. TITLE *(and Subtitle)*<br>Monopulse Angle Estimation from Coherently Integrated Radar Signals | | 5. TYPE OF REPORT & PERIOD COVERED<br>Technical Report<br>6. PERFORMING ORG. REPORT NUMBER<br>Technical Report 619 |
| 7. AUTHOR(s)<br>Robert E. Nicholls | | 8. CONTRACT OR GRANT NUMBER(s)<br>F19628-80-C-0002 |
| 9. PERFORMING ORGANIZATION NAME AND ADDRESS<br>Lincoln Laboratory, M.I.T.<br>P.O. Box 73<br>Lexington, MA 02173-0073 | | 10. PROGRAM ELEMENT, PROJECT, TASK AREA & WORK UNIT NUMBERS<br>Program Element Nos.<br>63304A/63308A |
| 11. CONTROLLING OFFICE NAME AND ADDRESS<br>Ballistic Missile Defense Program Office<br>Department of the Army<br>5001 Eisenhower Avenue<br>Alexandria, VA 22333 | | 12. REPORT DATE<br>25 August 1982<br>13. NUMBER OF PAGES<br>30 |
| 14. MONITORING AGENCY NAME & ADDRESS *(if different from Controlling Office)*<br>Electronic Systems Division<br>Hanscom AFB, MA 01731 | | 15. SECURITY CLASS. *(of this report)*<br>Unclassified<br>15a. DECLASSIFICATION DOWNGRADING SCHEDULE |

16. DISTRIBUTION STATEMENT *(of this Report)*

Approved for public release, distribution unlimited.

17. DISTRIBUTION STATEMENT *(of the abstract entered in Block 20, if different from Report)*

18. SUPPLEMENTARY NOTES

None

19. KEY WORDS *(Continue on reverse side if necessary and identify by block number)*

deep space radar | monopulse estimation | coherent detection

20. ABSTRACT *(Continue on reverse side if necessary and identify by block number)*

A maximum likelihood estimator is derived for monopulse radar signals which have been coherently integrated. Field data from the Millstone Hill radar is reduced using the estimator and the results are compared with known values derived from an accurately computed ephemeris.

DD FORM 1 Jan 73 1473 EDITION OF 1 NOV 65 IS OBSOLETE

UNCLASSIFIED

SECURITY CLASSIFICATION OF THIS PAGE *(When Data Entered)*